Supporting Information

Hg^{2+}-Reactive Double Hydrophilic Block Copolymer Assemblies as Novel Multifunctional Fluorescent Probes with Improved Performance

Jinming Hu, Changhua Li, and Shiyong Liu*

CAS Key Laboratory of Soft Matter Chemistry, Department of Polymer Science and Engineering, Hefei National Laboratory for Physical Sciences at the Microscale, University of Science and Technology of China, Hefei, Anhui 230026, China

***** To whom correspondence should be addressed. E-mail: sliu@ustc.edu.cn

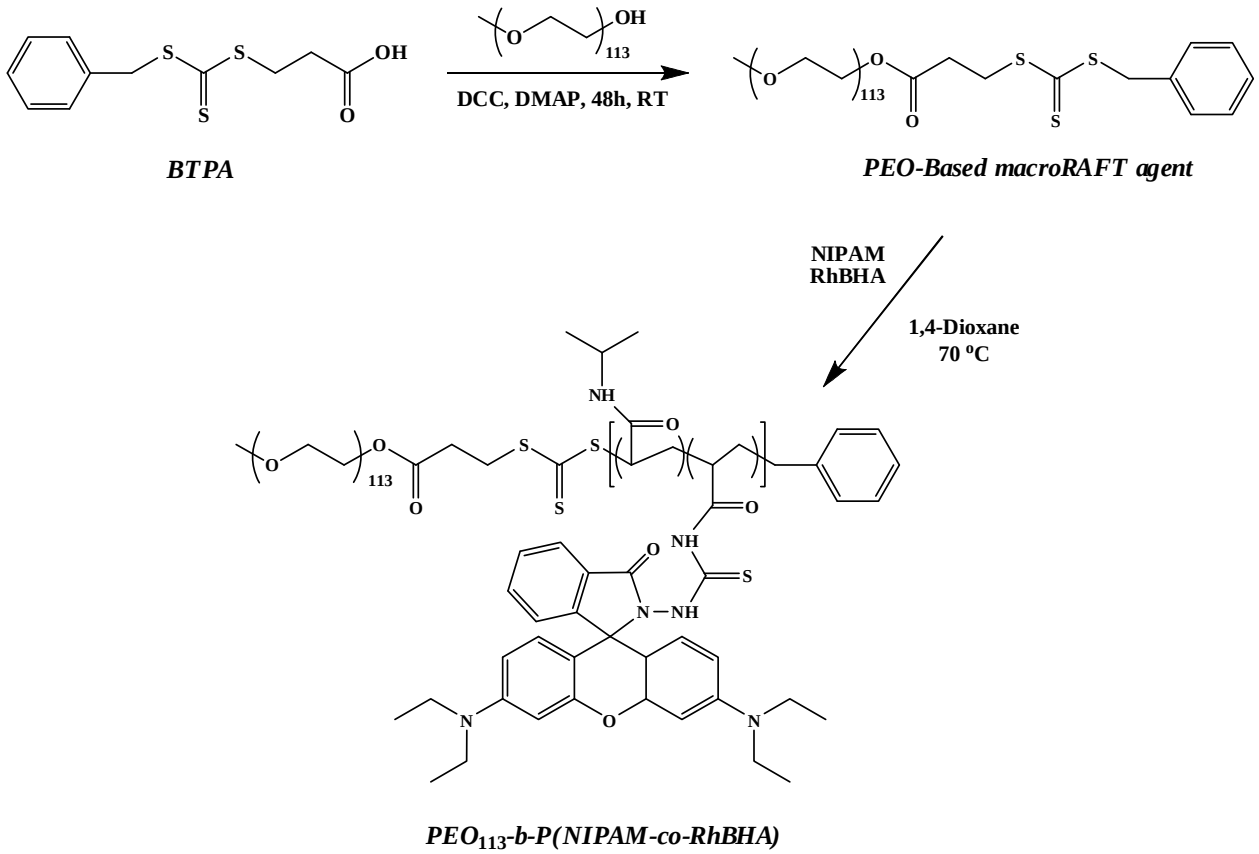

Scheme S1. Schematic for the RAFT synthesis of well-defined double hydrophilic block copolymer bearing RhBHA moieties, PEO-*b*-P(NIPAM-*co*-RhBHA).

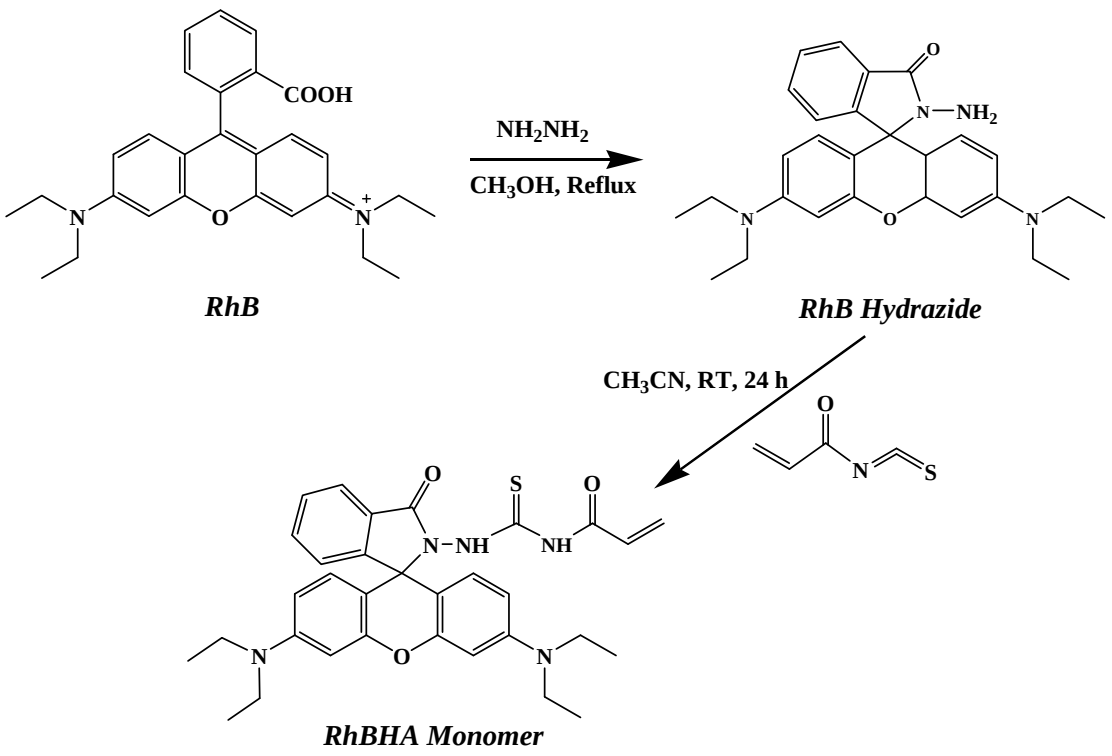

Scheme S2. Schematic for the synthesis of rhodamine B-based spirolactam monomer (RhBHA).

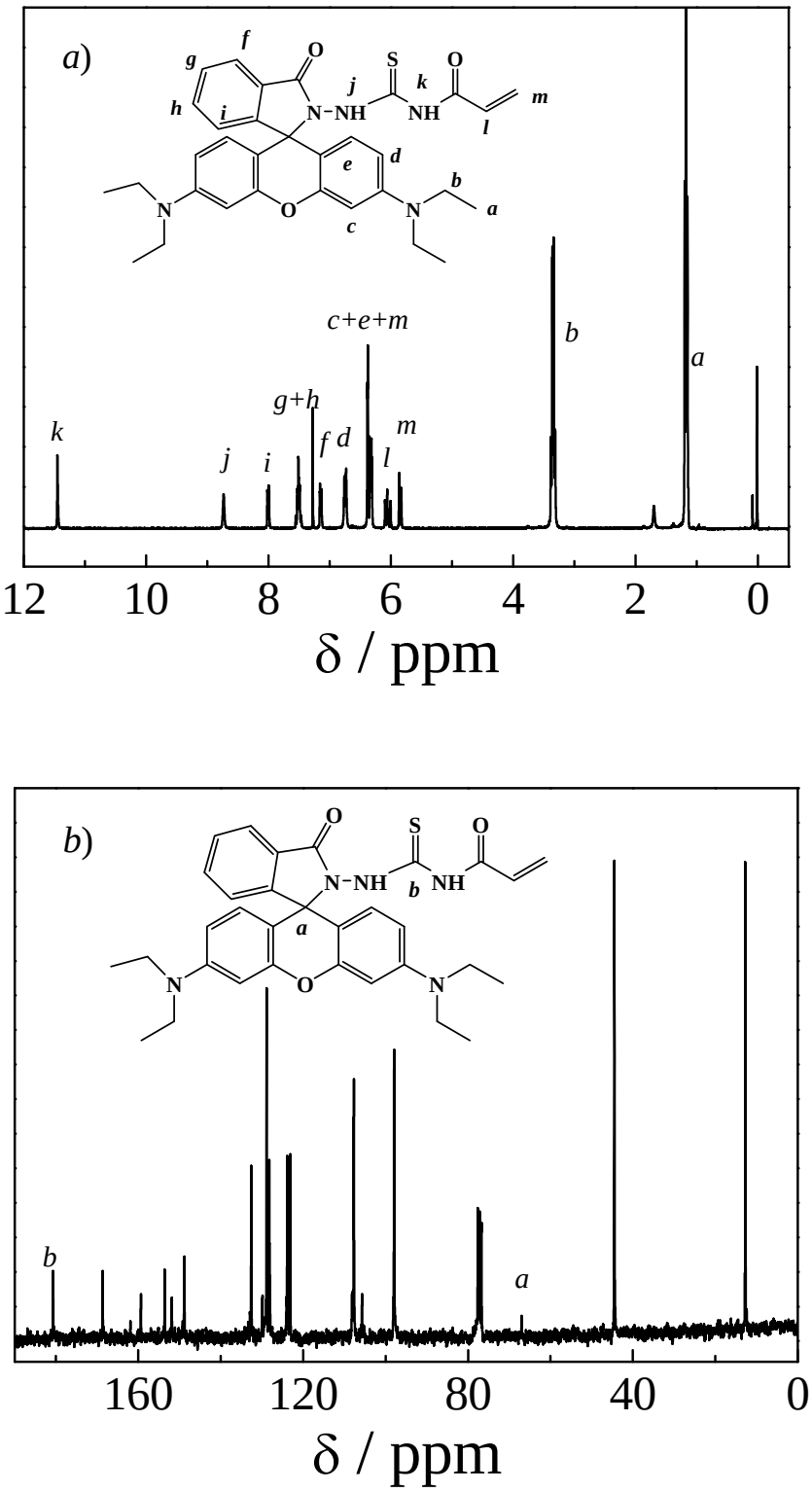

Figure S1. (a) ^{1}H NMR and (b) ^{13}C NMR spectra recorded for rhodamine B-based monomer, RhBHA, in $CDCl_3$.

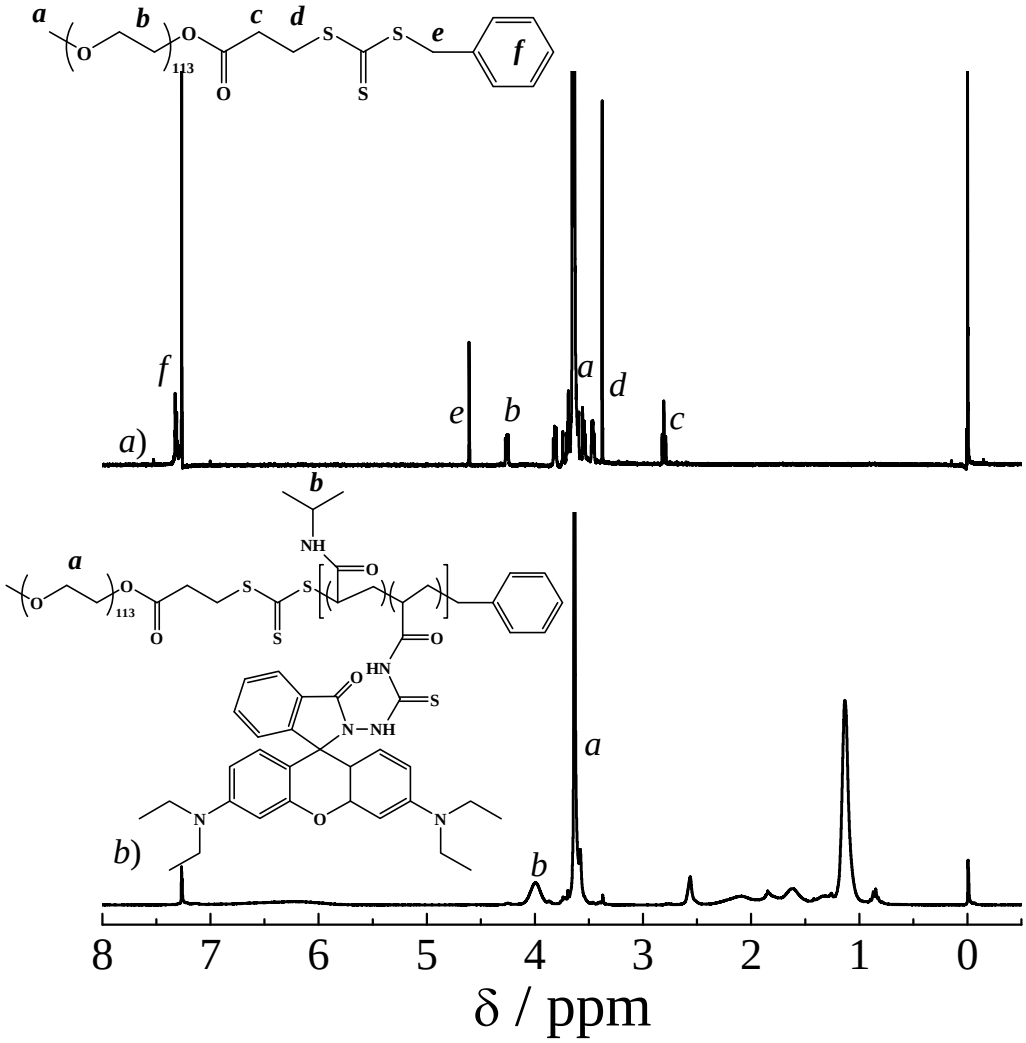

Figure S2. ^{1}H NMR spectra recorded for (a) PEO-based macroRAFT agent and (b) PEO_{113}-*b*-P(NIPAM-*co*-RhBHA)$_{69}$.

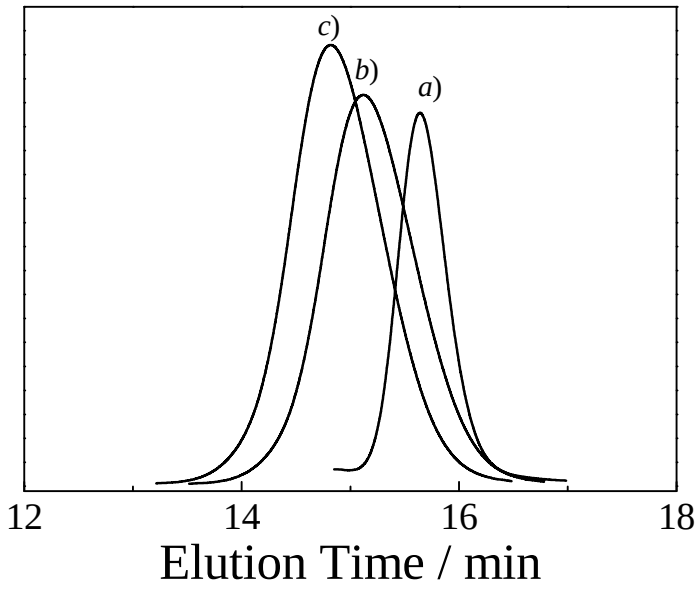

Figure S3. THF GPC traces recorded for (a) PEO-based macroRAFT agent, (b) PEO_{113}-*b*-P(NIPAM-*co*-RhBHA)$_{69}$, and (c) PEO_{113}-*b*-P(NIPAM-*co*-RhBHA)$_{115}$ double hydrophilic block copolymers (DHBCs).

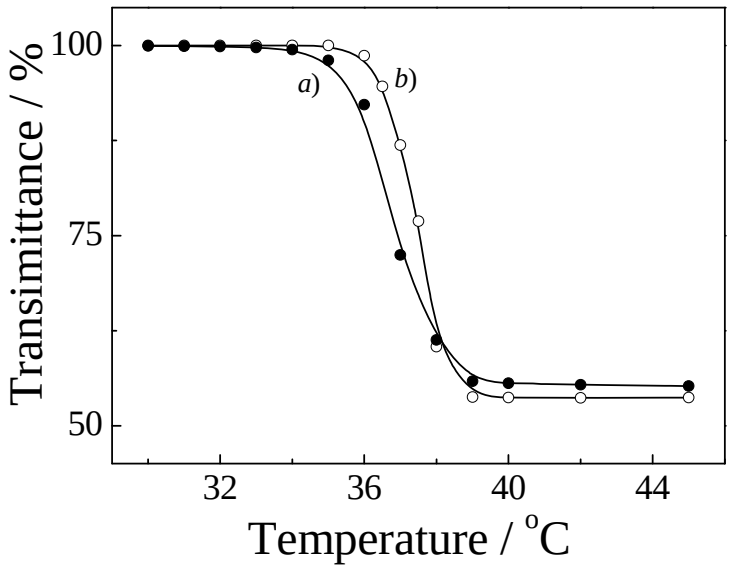

Figure S4. Temperature-dependence of optical transmittance recorded at a wavelength of 800 nm for 0.1 g/L aqueous solutions of (a) PEO_{113}-*b*-P(NIPAM-*co*-RhBHA)$_{115}$ and (b) PEO_{113}-*b*-P(NIPAM-*co*-RhBHA)$_{69}$ diblock copolymers.

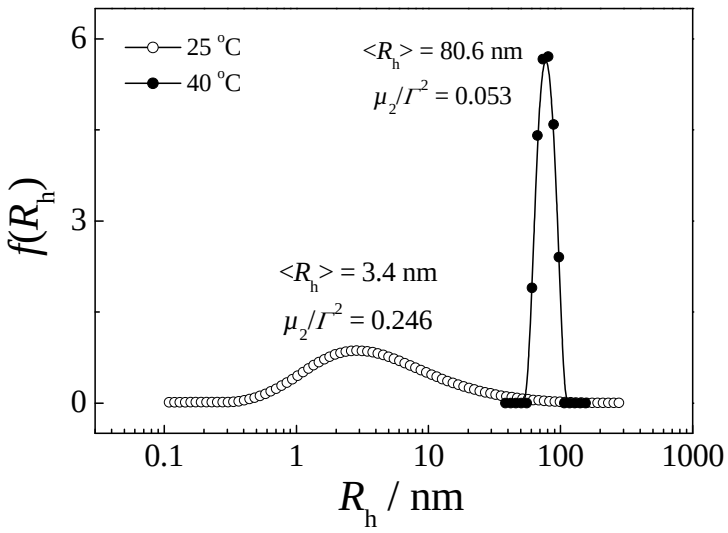

Figure S5. Hydrodynamic radius distributions, $f(R_h)$, obtained for 0.1 g/L aqueous solution of PEO_{113}-*b*-P(NIPAM-*co*-RhBHA)$_{69}$ diblock copolymer at 25 ^{o}C and 40 ^{o}C, respectively.

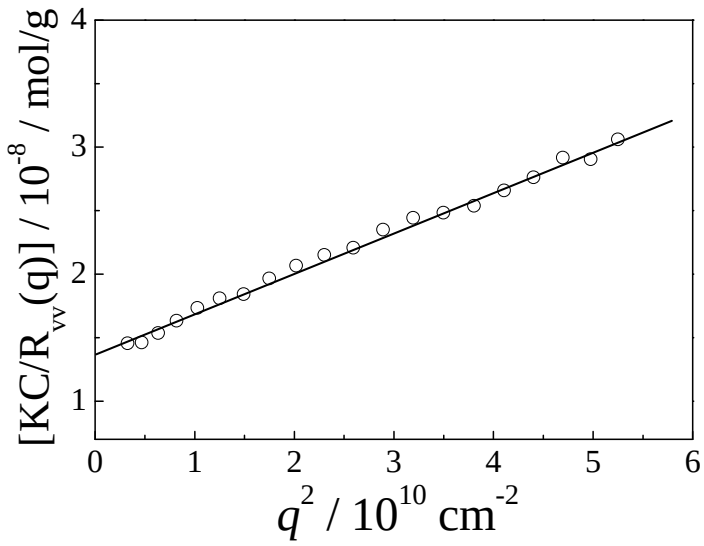

Figure S6. Scattering vector (q) dependence of Rayleigh ratio, $R_{vv}(q)$, recorded for 0.1 g/L aqueous solution of PEO_{113}-*b*-P(NIPAM-*co*-RhBHA)$_{69}$ diblock copolymer at 40 ^{o}C.

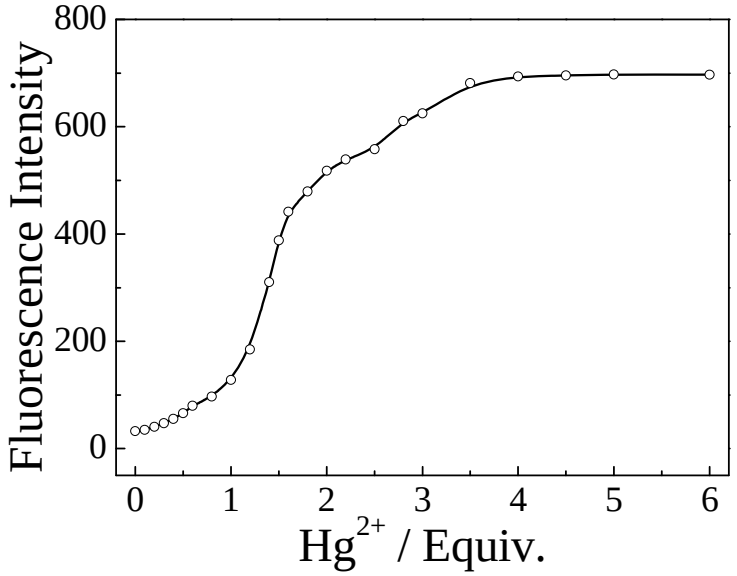

Figure S7. Change in fluorescence intensity (λ_{em} = 584 nm) of 0.05 g/L aqueous solution of PEO_{113}-*b*-P(NIPAM-*co*-RhBHA)$_{69}$ (pH 7, 25 ^{o}C; [RhBHA] = 1.25 μM; λ_{ex} = 500 nm, slit widths: Ex. 5 nm, Em. 5 nm) upon gradual addition of Hg^{2+} (0-5 equiv.).

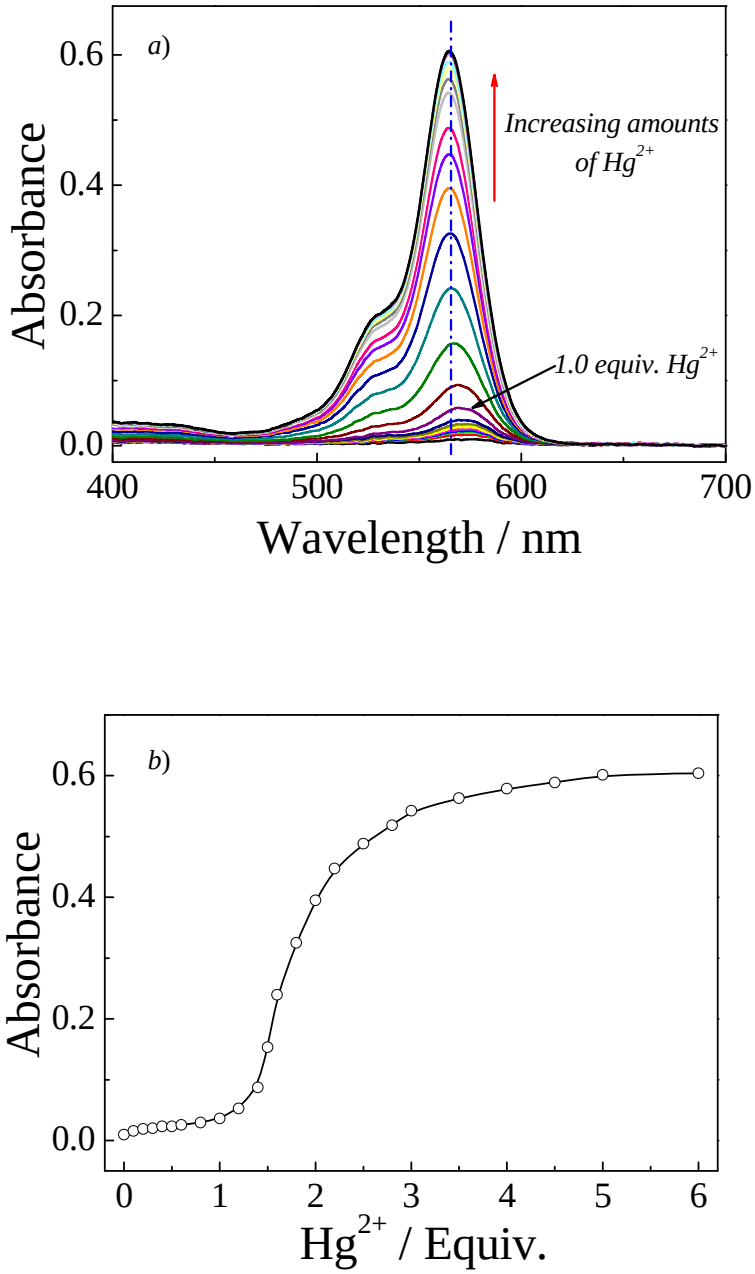

Figure S8. (a) UV-Vis absorbance spectra and (b) absorbance intensity (λ_{max} = 565 nm) changes recorded for 0.05 g/L aqueous solution of PEO_{113}-*b*-P(NIPAM-*co*-RhBHA)$_{69}$ (pH 7, 25 ^{o}C; [RhBHA] = 1.25 μM) upon gradual addition of Hg^{2+} (0-5 equiv.).

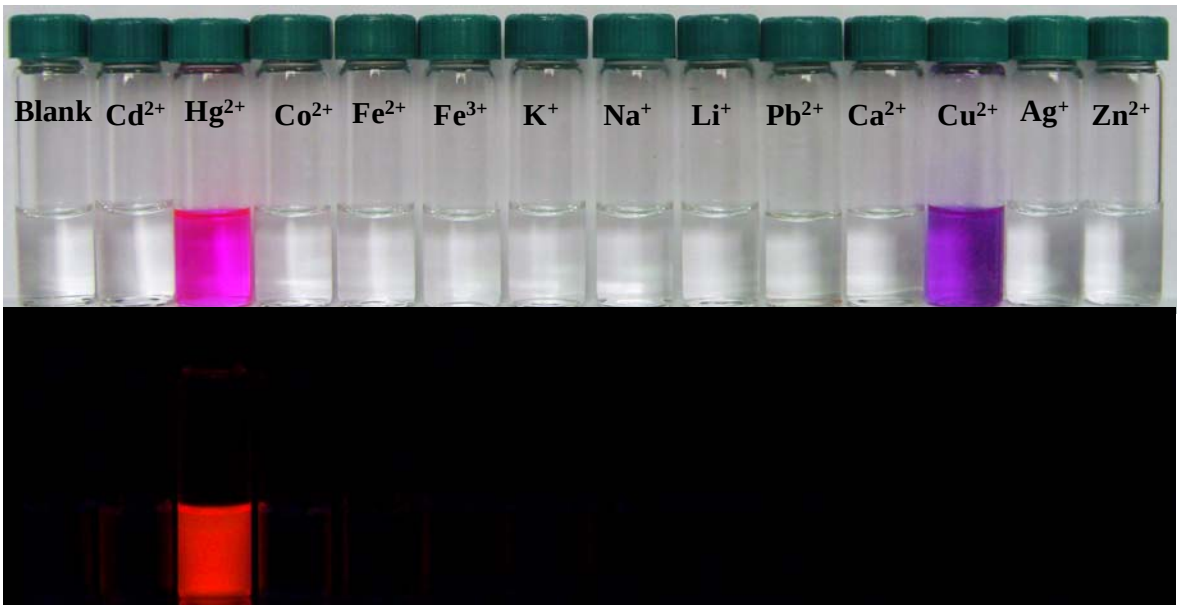

Figure S9. Optical photographs recorded under visible light (top) and UV (365 nm, bottom) for aqueous solutions (pH 7, 25 ^{o}C) of PEO_{113}-*b*-P(NIPAM-*co*-RhBHA)$_{69}$ within 10 mins upon addition of 5 equiv. of Cd^{2+}, Hg^{2+}, Co^{2+}, Fe^{2+}, Fe^{3+}, K^{+}, Na^{+}, Li^{+}, Pb^{2+}, Ca^{2+}, Cu^{2+}, Ag^{+}, and Zn^{2+}, respectively.

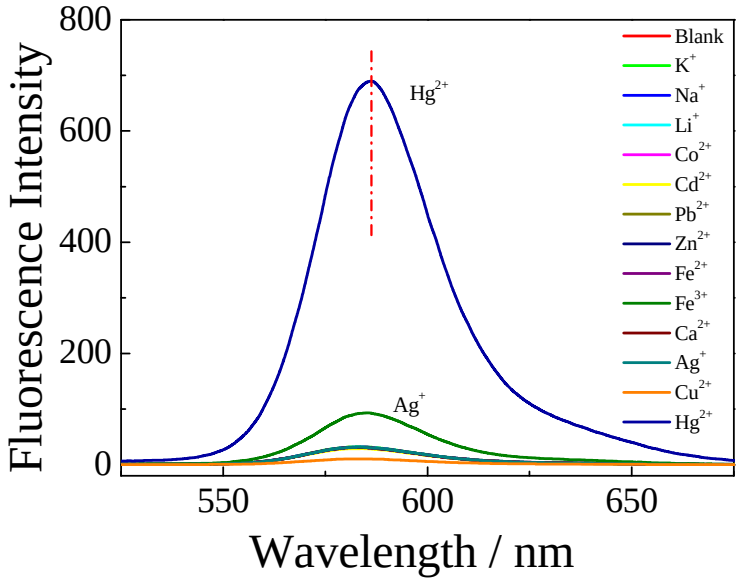

Figure S10. Fluorescence emission spectra (λ_{ex} = 500 nm, slit widths: Ex. 5 nm, Em. 5 nm) recorded for 0.05 g/L aqueous solution of PEO_{113}-*b*-P(NIPAM-*co*-RhBHA)$_{69}$ (pH 7, 25 ^{o}C; [RhBHA] = 1.25 μM) within 5 h after the addition of 5 equiv. of K^+, Na^+, Li^+, Co^{2+}, Cd^{2+}, Pb^{2+}, Zn^{2+}, Fe^{2+}, Fe^{3+}, Ca^{2+}, Ag^+, Cu^{2+}, and Hg^{2+} ions, respectively.

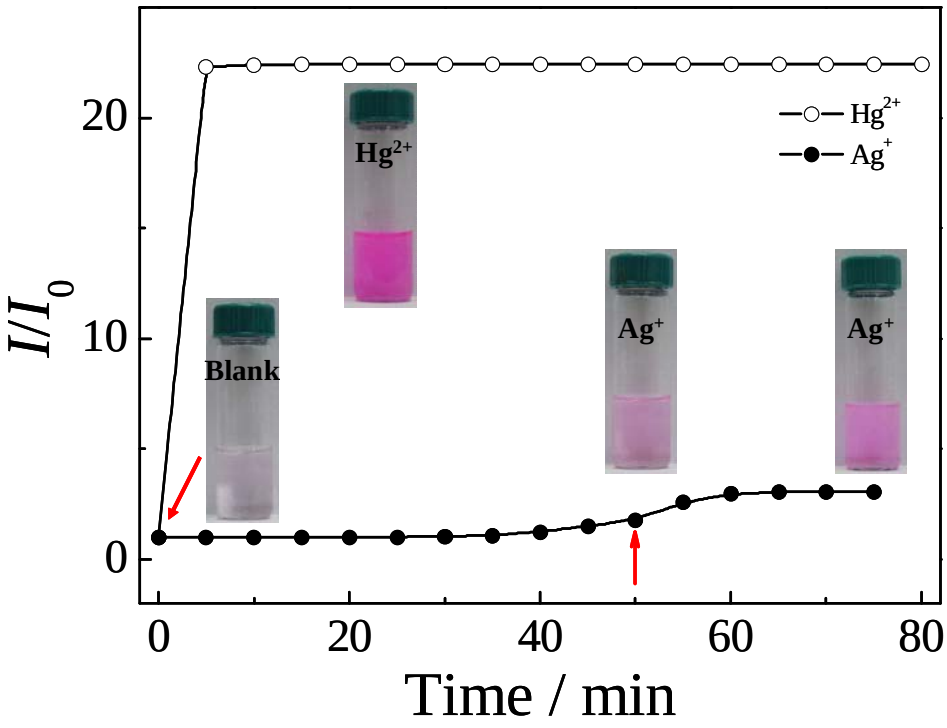

Figure S11. Time-dependence of relative fluorescence intensity (λ_{ex} = 500 nm, slit widths: Ex. 5 nm, Em. 5 nm) recorded for 0.05 g/L aqueous solutions of PEO_{113}-*b*-P(NIPAM-*co*-RhBHA)$_{69}$ (pH 7, 25 ^{o}C) upon addition of 5 equiv. of Ag^{+} and Hg^{2+} ions, respectively.

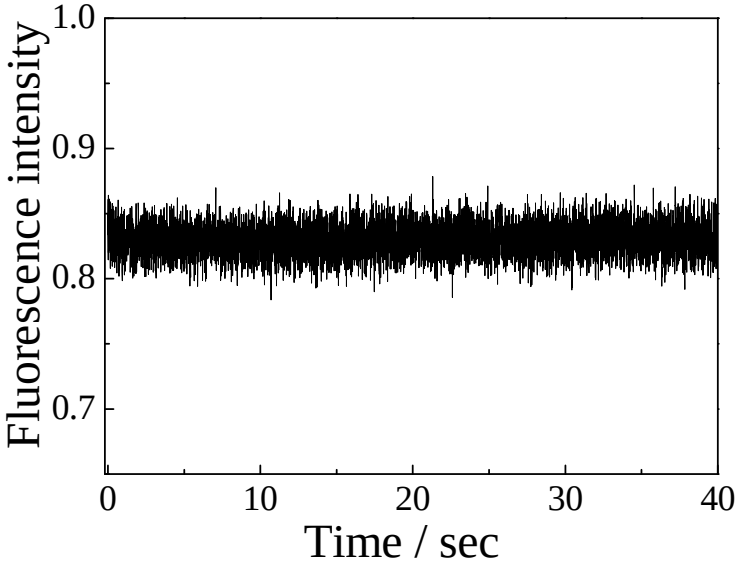

Figure S12. Time-dependence of fluorescence emission intensity (λ_{ex} = 500 nm, λ_{em} = 584 nm; slit widths: Ex. 10 nm, Em. 10 nm) recorded upon stopped-flow mixing 0.05 g/L aqueous solution (pH 7, 25 ^{o}C) of PEO_{113}-*b*-P(NIPAM-*co*-RhBHA)$_{69}$ with 5 equiv. of Hg^{2+} ions.

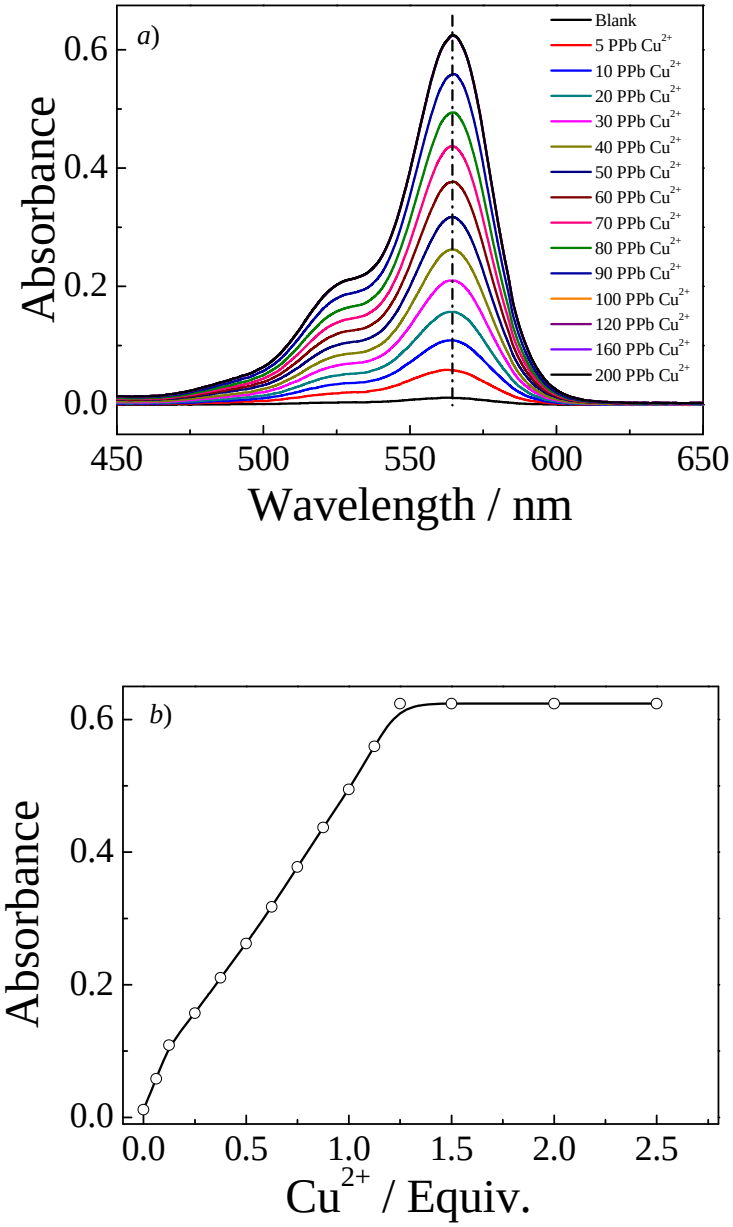

Figure S13. (a) UV-Vis absorbance spectra and (b) change in absorbance intensity (λ_{max} = 564 nm) recorded for 0.05 g/L aqueous solution of PEO_{113}-*b*-P(NIPAM-*co*-RhBHA)$_{69}$ (pH 7, 25 ^{o}C; [RhBHA] = 1.25 μM) upon gradual addition of Cu^{2+} ions (0-2.5 equiv.).

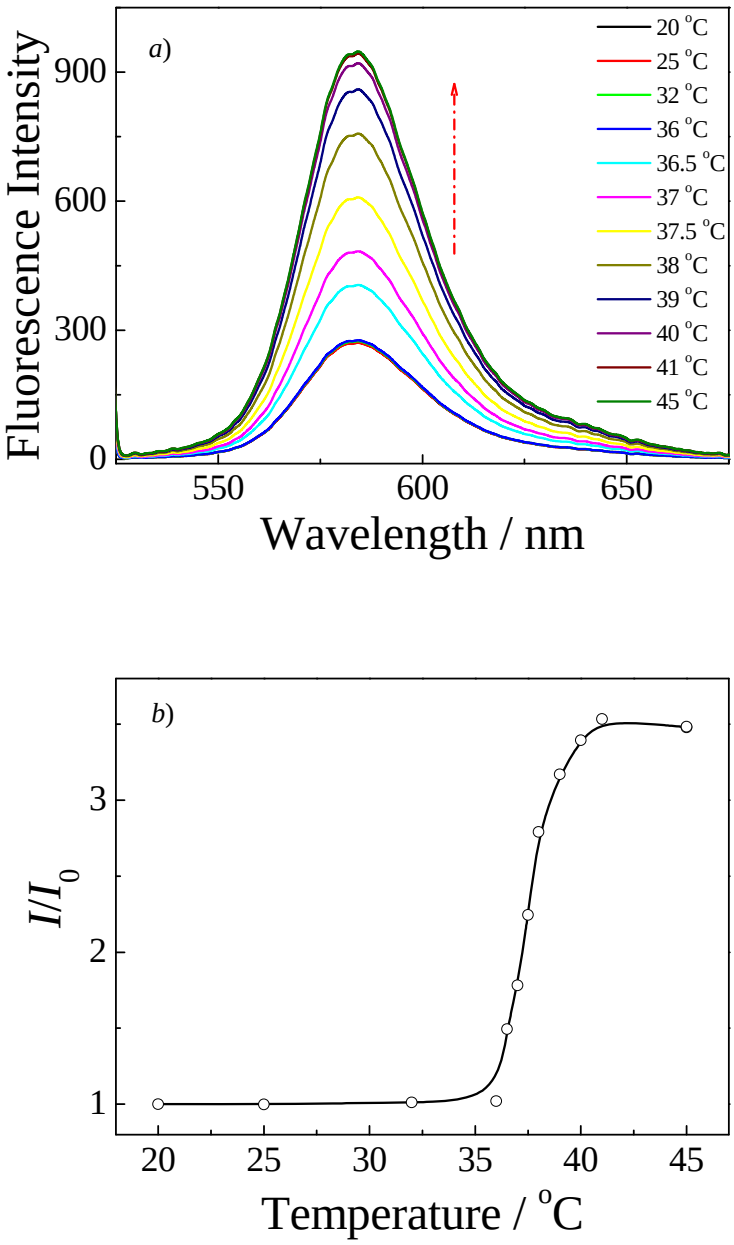

Figure S14. (a) Fluorescence spectra and (b) change in relative fluorescence intensity (λ_{ex} = 500 nm, slit widths: Ex. 5 nm, Em. 3 nm) recorded for 0.05 g/L aqueous solution of PEO_{113}-*b*-P(NIPAM-*co*-RhBHA)$_{69}$ (pH 7 and 5 equiv. Hg^{2+}) in the temperature range of 20-45 °C.

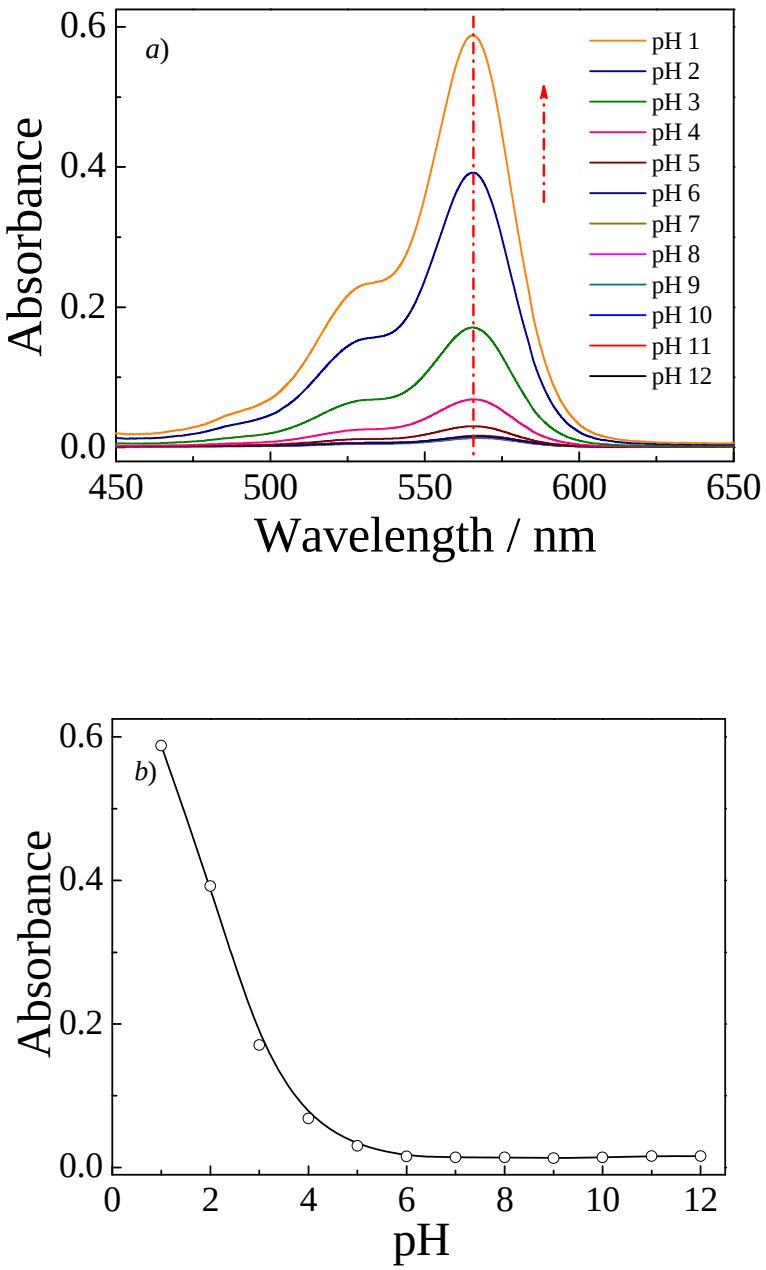

Figure S15. (a) Absorbance spectra and (b) change in absorbance intensity at 565 nm recorded for 0.05 g/L aqueous solution of PEO_{113}-*b*-P(NIPAM-*co*-RhBHA)$_{69}$ (25 ^{o}C) in the pH range of 1-12.

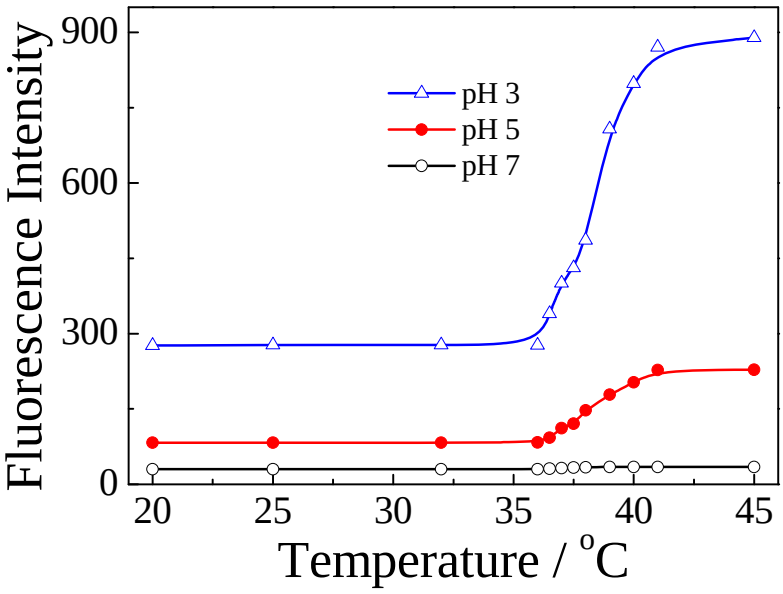

Figure S16. Change in fluorescence emission intensity (λ_{ex} = 500 nm, λ_{em} = 584 nm; slit widths: Ex. 5 nm, Em. 3 nm) recorded for 0.05 g/L PEO_{113}-*b*-P(NIPAM-*co*-RhBHA)$_{69}$ at pH 3, pH 5, and pH 7 in the temperature range of 20-45 ^{o}C.